Journal of Cellular Biochemistry 84:625–635 (2002)

Expression of Na^+/Ca^{2+} Exchanger Isoforms (NCX1 and NCX3) and Plasma Membrane Ca^{2+} ATPase During Osteoblast Differentiation

Joseph P. Stains, Janet A. Weber, and Carol V. Gay*

Department of Biochemistry and Molecular Biology, The Pennsylvania State University, University Park, Pennsylvania 16802

Abstract The ability to deliver calcium to the osteoid is critical to osteoblast function as a regulator of bone calcification. There are two known transmembrane proteins capable of translocating calcium out of the osteoblast, the Na^+/Ca^{2+} exchanger (NCX) and the plasma membrane Ca^{2+}-ATPase (PMCA). In this study, we reveal the presence of the NCX3 isoform in primary osteoblasts and examine the expression of NCX1, NCX3, and PMCA1 during osteoblast differentiation. The predominant NCX isoform expressed by osteoblasts is NCX3. NCX1 also is expressed, but at low levels. Both NCX isoforms are expressed at nearly static levels throughout differentiation. In contrast, PMCA expression peaks at 8 days of culture, early in osteoblast differentiation, but declines thereafter. Immunocytochemical co-detection of NCX and PMCA reveal that NCX is positioned along surfaces of the osteoblast adjacent to osteoid, while PMCA is localized to plasma membrane sites distal to the osteoid. The expression pattern and spatial distribution of NCX support a role as a regulator of calcium efflux from osteoblasts required for calcification. The expression pattern and spatial distribution of PMCA makes its role in the mineralization process unlikely and suggests a role in calcium homeostasis following signaling events. J. Cell. Biochem. 84: 625–635, 2002.

Key words: Na^+/Ca^{2+} exchanger; plasma membrane Ca^{2+} ATPase; mineralization; osteoblasts; cell polarity

The skeleton is a major reservoir for calcium. Calcium is deposited as a phosphate salt into bone matrix formed by osteoblasts and is removed from bone by osteoclastic bone degradation and osteocytic osteolysis. Maintenance of skeletal homeostasis requires a balance between osteoblast-mediated bone formation and osteoclast-controlled bone resorption. Currently, the mechanisms utilized by the osteoblast to regulate mineralization are poorly understood.

Osteoblasts contain two calcium efflux mechanisms, the plasma membrane Ca^{2+}-ATPase (PMCA) [Shen et al., 1983; Anderson et al., 1984] and the Na^+/Ca^{2+} exchanger (NCX) [Krieger and Tashjian, 1980; Krieger, 1992; White et al., 1996]. PMCA has been suggested to play a key role in bone mineralization [Abramowitz and Suki, 1996], and offers the attractive advantage of being a highly specific, outwardly directed transporter for Ca^{2+} [Carafoli, 1991]. Three isoforms of PMCA have been found in osteoblastic cells, primarily PMCA1, but also PMCA2 and PMCA4 [Meszaros and Karin, 1993; Abramowitz et al., 1995]. Additionally, PMCA is known to interact with the calcium binding protein, calmodulin [Jarrett and Penniston, 1977; Graf and Penniston, 1981; Gmaj et al., 1982], a well-established Ca^{2+} dependent regulatory peptide. Interestingly, cytochemical techniques used to localize PMCA in osteoblasts have shown it to be distributed along the plasma membrane of the osteoblast on the marrow-facing side of the cell, distal to the bone matrix [Akisaka et al., 1988; Watson et al., 1989]. As a consequence, a direct role of PMCA in mineralization is unlikely.

The first indication of NCX, a Na^+ gradient driven antiporter, in bone came from organ culture experiments by Krieger and Tashjian [1980]. Subsequent reports have revealed the presence of such a mechanism in primary mouse osteoblasts and an osteoblast-like cell

Grant sponsor: NIH; Grant number: DE 09459.

*Correspondence to: Dr. Carol V. Gay, The Pennsylvania State University, 108 Althouse Lab, University Park, PA 16802. E-mail: cvg1@psu.edu

Received 13 July 2001; Accepted 9 October 2001

DOI 10.1002/jcb.10050

line [Krieger, 1992, 1997; Short et al., 1994]. The NCX1 isoform has been described in UMR 106 cells, a rat osteoblast-like cell line [White et al., 1996]. The function of NCX in osteoblasts has yet to be completely established. In other tissues it serves as a low affinity, high capacity translocator for Ca^{2+} [Carafoli, 1991]. The presence of functional NCX has been demonstrated on the osteoid-facing side of osteoblasts [Stains and Gay, 1998]. Specific inhibition of NCX prevents mineralization in vitro [Stains and Gay, 2001].

In this study, we examine the expression and localization of the Ca^{2+} efflux proteins, NCX and PMCA, to determine if the expression and deployment are consistent with a role in osteoblast-mediated calcification. We report here the first indication of the presence of NCX3 in osteoblasts. Further, we find that both the expression and cellular localization of NCX is consistent with a possible role in mineralization, while PMCA expression and cellular distribution makes it unlikely to play a direct role in calcification.

MATERIALS AND METHODS

Osteoblast Isolation and Culture

Primary osteoblasts were isolated from the tibias of 2-week-old chickens, as described previously [Gay et al., 1994]. Briefly, osteoblasts were obtained from chick tibias by mild sequential enzymatic digestion, followed by scraping the periosteal surface of the bone with a curette. Cells were cultured for up to 20 days in Dulbecco's modified Eagle's medium (DMEM, Sigma, St. Louis, MO) supplemented with 3.7 g/L sodium bicarbonate, 0.05 g/L ascorbate, 100 U/L penicillin, 100 mg/L streptomycin, and 10% fetal bovine serum (Sigma). After 48 h in culture, the cultures were rinsed in DMEM to remove any residual bone particles. On alternate days, half of the media was replaced with fresh media. Once the osteoblasts reached confluence at the sixth day of culture, the medium was supplemented with 10 mM β-glycerophosphate.

Alkaline Phosphatase (ALP) Staining

ALP activity was examined qualitatively by staining cultured osteoblasts with 10 μM napthol-AS-BI-phosphate in 100 mM Tris, pH 8.5, plus 0.06% fast blue RR for 20 min at 37°C. The formation of a blue precipitate indicates ALP activity.

ALP activity was quantitated using an ALP-10 kit (Sigma) that monitors the conversion of *p*-nitrophenol phosphate to *p*-nitrophenol by measuring the OD at 405 nm. Osteoblasts cultured for 4, 8, 12, 16, or 20 days, were rinsed twice in phosphate buffered saline (PBS), resuspended in 100 μl of 100 mM glycine, 1 mM $MgCl_2$, 0.1% Triton-X-100, pH 10.0, and incubated on ice for 10 min. Samples were stored at -80°C until all data points were gathered. The samples were thawed and 20 μl added to 1 ml of the *p*-nitrophenol phosphate containing assay reagent. The OD at 405 nm was measured at 1 min and at 3 min. ALP activity was calculated using the change in OD at 405 nm divided by the mM extinction coefficient of *p*-nitrophenol (18.45). Specific activity was determined by dividing the activity by the protein concentration of the samples as determined by the BCA assay (Pierce Chemical Co., Rockford, IL).

Assessment of Mineralization

Qualitative observation of mineralization by osteoblasts was made by von Kossa staining [Humason, 1967]. Cultured osteoblasts were rinsed in PBS and fixed for 10 min in 10% neutral-buffered formalin. The cells were incubated in the dark for 30 min in 5% silver nitrate, rinsed three times in distilled water, and then exposed to ambient light for color development. A dark black/brown precipitate is indicative of positive staining for deposited mineral.

Mineralization by osteoblasts was quantitated according to the method of Gronowicz et al. [1989]. Coverslips, at selected time points, were washed three times in PBS for 5 min each to remove aqueous Ca^{2+}. Mineral deposited by the cultured cells was solubilized by two 1-h incubations in 250 μl of 5% trichloroacetic acid (TCA). Ca^{2+} content was assessed using an *o*-cresolphthalein-based calcium quantitation kit (Sigma Diagnostics). The TCA extracts were pooled and then a 10 μl aliquot or vehicle (5% TCA) was added to 1 ml of calcium binding reagent working solution. The reaction was incubated at room temperature for 10 min and the OD at 575 nm measured. Calcium/phosphate combined standards were purchased from Sigma and were used to plot a standard curve for determining the Ca^{2+} content of the experimental samples.

Immunoblotting for NCX and PMCA

Plasma membrane fractions were prepared as described previously [Gay and Lloyd, 1995]. The procedure was modified in that the use of collagenase was omitted and all steps included the presence of a protease inhibitor cocktail containing 0.5 mM EDTA, 1 μg/ml leupeptin, 1 μg/ml pepstatin, and 1 mM phenylmethylsulfonylfluoride (PMSF). Briefly, osteoblasts cultured on 100-mm plates were removed from the surface of the plate into PBS by scraping with a rubber policeman. The cells were pelleted at 600*g* for 10 min, resuspended in 4 ml H_2O, and sonicated three times for 1 min each to lyse the cells. The samples were centrifuged at 930*g* and then the supernatant centrifuged at 10,000*g*. The supernatant was then applied to a 20% Percoll gradient and centrifuged at 46,000*g* for 30 min. The resulting plasma membrane fraction, present as an opaque, fluffy layer near the top of the Percoll gradient, was aspirated and stored at −80°C until needed.

SDS–PAGE was performed according to the method of Laemmli [1970]. Protein concentration of the plasma membrane fraction was determined by the BCA assay (Pierce, Rockford, IL). Protein samples were electrophoresed on 7.5% polyacrylamide gels and then transferred onto Immobilon-P polyvinylidene fluoride (PVDF) membrane (Millipore, Corp., Bedford, MA). Membranes were blocked in 5% non-fat dry milk in Tris-buffered saline with 0.1% Tween 20 (TBS-T). Primary antibodies were applied at a dilution of 1:1,000 for both rabbit anti-canine cardiac sarcolemmal NCX polyclonal antibodies (Research Diagnostics, Inc., Flanders, NJ) and mouse anti-plasma membrane Ca^{2+}-ATPase antibodies (PMCA; Research Diagnostics, Inc.); mouse anti-β actin monoclonal antibodies (Sigma) were used at a 1:5,000 dilution. Actin signal was used as a loading control. After rinsing with TBS-T, the blots were incubated in horseradish peroxidase (HRP) linked mouse or rabbit antibodies at a dilution of 1:5,000. Immunoreactions were detected using the ECL Western blotting analysis system (Amersham International, Cleveland, OH).

Relative Quantitative RT-PCR

Total RNA was isolated from osteoblasts cultures using TRIzol reagent (Life Technologies, Rockville, MD). Two micrograms of total RNA was reverse transcribed from random decamers using the RETROscript kit (Ambion, Austin, TX). One-tenth of this cDNA was then used for relative PCR to determine the levels of NCX and PMCA. Levels of amplified signal were normalized to 18S RNA, using QuantumRNA classic or alternate 18S internal standards (Ambion). PCR was optimized by varying the numbers of cycles to determine the linear range of amplification. The ratio of 18S primers and 18S competimers were selected so that the amount of 18S RNA PCR product is also linear under the same amplification conditions as the gene specific primers. RNA that had not been reverse transcribed was used as a negative control in each PCR reaction.

PCR of NCX1 was performed using the sense primer 5′-GTT GTT CCT GAT GGA GAA ATA AGG-3′ and the antisense primer 5′-TGG CCA AGA GAT ACT CGA CG-3′. These primers yield a product of 483 bp, corresponding to nucleotides 269–752 of the published chicken NCX1 sequence (GenBank accession number AJ012579). Alternate 18S internal standards and competimer were used at a 2:8 ratio. The PCR conditions were: one cycle at 94°C for 3 min, then 32 repetitions of 94°C for 30 s, 60°C for 30 s, and 72°C for 60 s. Chicken cardiac cDNA was used as a positive control for NCX1.

PCR of NCX2 was attempted using primers designed to conserved regions of the mammalian NCX2 gene, since chicken NCX2 had not been cloned [Quednau et al., 1997]. The sense primer was 5′-GCG TGT GGG CGA TGC TCA-3′ and the antisense primer was 5′-GAC CTC GAG GCG ACA GTT C-3′. Theoretically, these primers should amplify a 528-bp product, corresponding to nucleotides 1455–1983 of the published NCX2 gene [Li et al., 1994]. Several PCR conditions were tested.

PCR of NCX3 was performed using the sense primer 5′-ACA ACA ACA ACC ATT CGG ATT T-3′ and the antisense primer 5′-CAA AGT GGA AAG AAG AAA AGC G-3′. These primers yield a product of 367 bp, corresponding to nucleotides 71–438 of the published chicken NCX3 sequence (GenBank accession number AJ012580). Classic 18S internal standards and competimer were used at a 3:7 ratio. The PCR conditions were: 94°C for 3 min, then 28 rounds at 94°C for 30 s, 60°C for 30 s, and 72°C for 60 s. Chicken brain cDNA (Clontech, Palo Alto, CA) was used as a positive control tissue for NCX3.

PCR of PMCA was performed using the sense primer 5′-GCC ATC TTC TGC ACA ATT GT-3′ and the antisense primer 5′-TCA GAG TGA TGT TTC CAA AC-3′. These primers yield a product of 644 bp, as described previously [Cai et al., 1993]. Classic 18S internal standards and competimer were used at a 1:9 ratio. The PCR conditions were: one cycle of 94°C for 3 min, then 37 repetitions at 94°C for 30 s, 50°C for 30 s, and 72°C for 60 s.

PCR samples were electrophoresed on a 2.0% agarose gel, stained with ethidium bromide, and the gel documented using an Eagle Eye II digital imaging system (Stratagene, La Jolla, CA). Gel quantitation was performed by volume quantitation using ImageQuant software (Molecular Dynamics, Sunnyvale, CA).

Immunolocalization of NCX and PMCA

Osteoblasts cultured for 8 days on 12-mm glass coverslips were rinsed in PBS and then fixed in 4% paraformaldehyde for 15 min. After rinsing, the cells were permeabilized for 5 min in PBS + 0.2 % Triton-X-100, then blocked for 1 h in PBS + 10% normal goat serum (NGS). This was followed by incubation with rabbit anti-NCX and mouse anti-PMCA antibodies diluted 1:200 and 1:500, respectively, in PBS + 1% NGS + 0.1% Tween-20 (Sigma). Non-immune rabbit and mouse IgG antibodies (Sigma) were applied at a dilution of 1:200 for negative control samples. Coverslips were rinsed three times for 10 min each in PBS + 1% NGS + 0.1% Tween-20. For the secondary antibodies, goat anti-rabbit conjugated BODIPY (Molecular Probes, Eugene, OR) and donkey anti-mouse Cy3 (Chemicon, Temecula, CA) were each used at a dilution 1:250. The coverslips were washed several times in PBS and then mounted on microscope slides with Fluoromount G mounting media (Southern Biotechnology Associates, Inc., Birmingham, AL). Images were collected using a Bio-Rad 1024 confocal microscope (488 and 568 nm laser lines) and analyzed using Bio-Rad LaserSharp software (Hercules, CA).

RESULTS

Osteoblast Differentiation

Osteoblasts were examined for several markers of differentiation in order to characterize their progression in vitro and to provide a framework for assessing potential roles for NCX and PMCA in mineralization. Two markers are routinely used to distinguish the level of differentiation in cultured osteoblasts, ALP activity and the ability of the cells to mineralize. ALP is markedly elevated as osteoblasts mature, and then it decreases slightly once calcification has begun [Gerstenfeld et al., 1987; Turksen and Aubin, 1991; Bianco et al., 1993]. The presence of mineral signifies that osteoblasts have matured and are fully functional.

Primary osteoblasts were cultured for 4, 8, 12, 16, or 20 days and examined both qualitatively and quantively for levels of ALP activity. Osteoblasts were stained for ALP activity using napthol-AS-BI phosphate and fast blue RR (Fig. 1A, inset). Positive staining for ALP is denoted by the formation of a blue precipitate. ALP staining is low and limited to small patches of cells in four day cultures. By day 8, staining for ALP increases in both area and intensity, peaking at approximately day 12. By day 20, nearly all cells were positive for ALP activity, but the overall intensity of staining is reduced compared to those at day 12. The levels of ALP activity were quantitated by monitoring the rate of change in absorbance at 405 nm observed when *p*-nitrophenol phosphate is converted to *p*-nitrophenol (Fig. 1A). Osteoblasts, after the indicated time in culture, were lysed and then monitored for the accumulation of *p*-nitrophenol over 3 min. As was seen in the qualitative assay, ALP activity rose steadily until approximately the 12th day in culture, followed by a characteristic slight decline in activity after day 12.

The ability of cultures to mineralize in vitro was assessed both qualitatively and quantitatively. Qualitative evaluation of mineralizing capacity was done by von Kossa staining on osteoblasts cultured for 4, 8, 12, 16, or 20 days. Mineralization is indicated by the formation of a dark brown or black precipitate (Fig. 1B, inset). The first appearance of significant mineral appeared at day 12. Mineral continued to accumulate through the 20 days that the cells were cultured. Quantitation of mineralization levels by measuring the acid soluble Ca^{2+} of osteoblasts cultures using the Ca^{2+} sensitive indicator, *o*-cresolpthalein, mirrored that of the von Kossa stained cultures (Fig. 1B). Mineral began to accumulate around day 12, and by day 20 the concentration of Ca^{2+} in the acid extracts were typically around 70 mM.

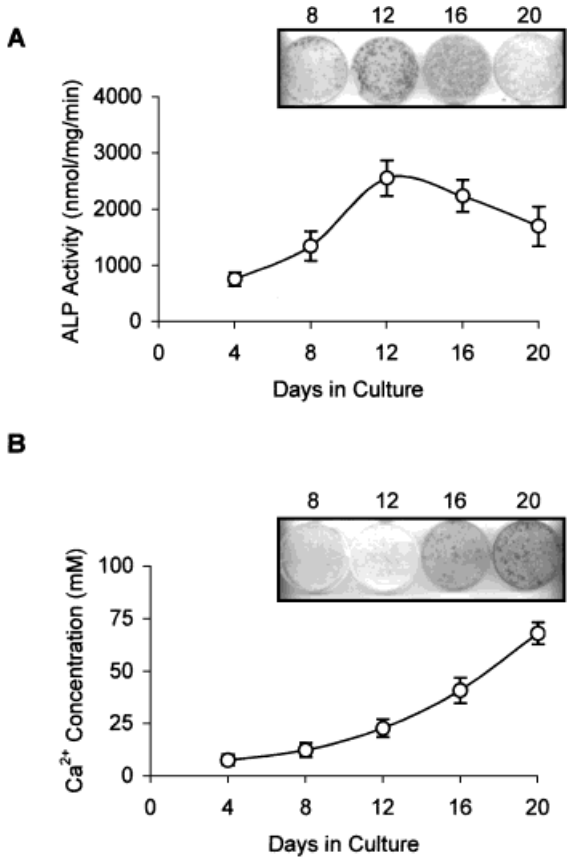

Fig. 1. **A**: ALP activity present in cultured osteoblasts. Quantitative measurement of ALP activity was made from osteoblasts cultured for the indicated times. The data are expressed as the mean ± standard deviation (n = 3). Inset, osteoblasts cultured in 60-mm dishes were stained for ALP activity using napthol-AS-BI-phosphate and fast blue RR following 8, 12, 16, or 20 days of culture. A blue precipitate indicates cells contained ALP activity. **B**: Mineralization by cultured osteoblasts. Quantitative measurement of mineralization was performed on osteoblasts cultured for the indicated times using an *o*-cresolpthalein based assay. The data are presented as the mean ± standard deviation (n = 3). Inset, osteoblasts cultured in 60-mm dishes for the indicated time points were stained by the von Kossa method. A dark black/brown precipitate is indicative of calcification.

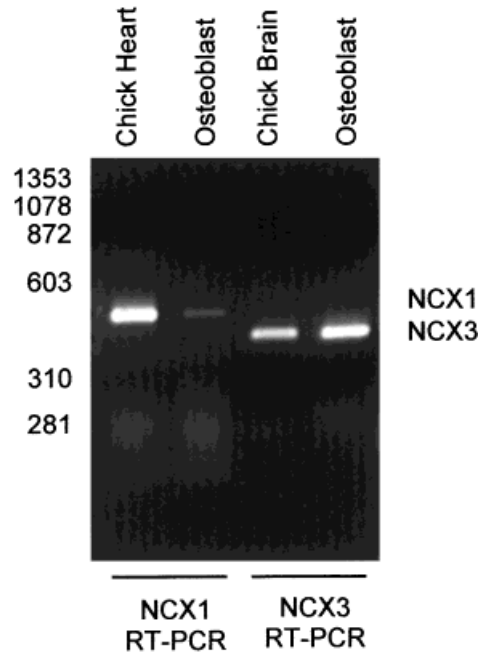

Fig. 2. Detection of NCX isoforms by RT-PCR. RNA isolated from 8-day osteoblasts, chicken heart, or chicken brain was reverse transcribed. RT-PCR products generated using isoform specific primers for chicken NCX1 and NCX3 were electrophoresed on a 2.0% agarose gel and stained with ethidium bromide. NCX1 expression was weakly detected as a 483-bp band by RT-PCR, while NCX3 was readily detected as a 367-bp product. Chicken heart and chicken brain cDNA were used as positive controls for NCX1 and NCX3, respectively. All reactions were performed under identical conditions over 28 rounds of amplification. Molecular weights (in bp) are indicated to the left.

NCX Isoform Expression

In order to determine which isoforms of NCX are present in avian osteoblasts, gene specific primers were designed to the sequenced chicken NCX genes, NCX1 and NCX3. chicken heart cDNA and chicken brain cDNA were used as a positive control for the presence of NCX1 and NCX3, respectively. RT-PCR with gene specific primers for NCX1 revealed only a weak product in osteoblasts (Fig. 2). NCX1 was abundant in chicken cardiac tissue. The NCX3 isoform of the exchanger was expressed in both cultured osteoblasts and in brain. The levels of NCX3 present in osteoblast cDNA appear greater than those detected for NCX1. NCX2 has not been described in avian cells, and therefore, could not be reliably tested. Attempts at PCR with conserved regions of mammalian derived sequences of NCX2 were unsuccessful (data not shown).

NCX and PMCA Expression

If NCX plays a role in mineralization, then NCX would be expected to be present when the cultured osteoblasts are actively mineralizing. Plasma membrane proteins were extracted from cells cultured at the selected time points. Immunoblots of the plasma membrane protein extracts probed with antibodies against the canine cardiac sarcolemmal NCX reveal that the exchanger is present throughout the time course of culture (Fig. 3A). The levels of NCX

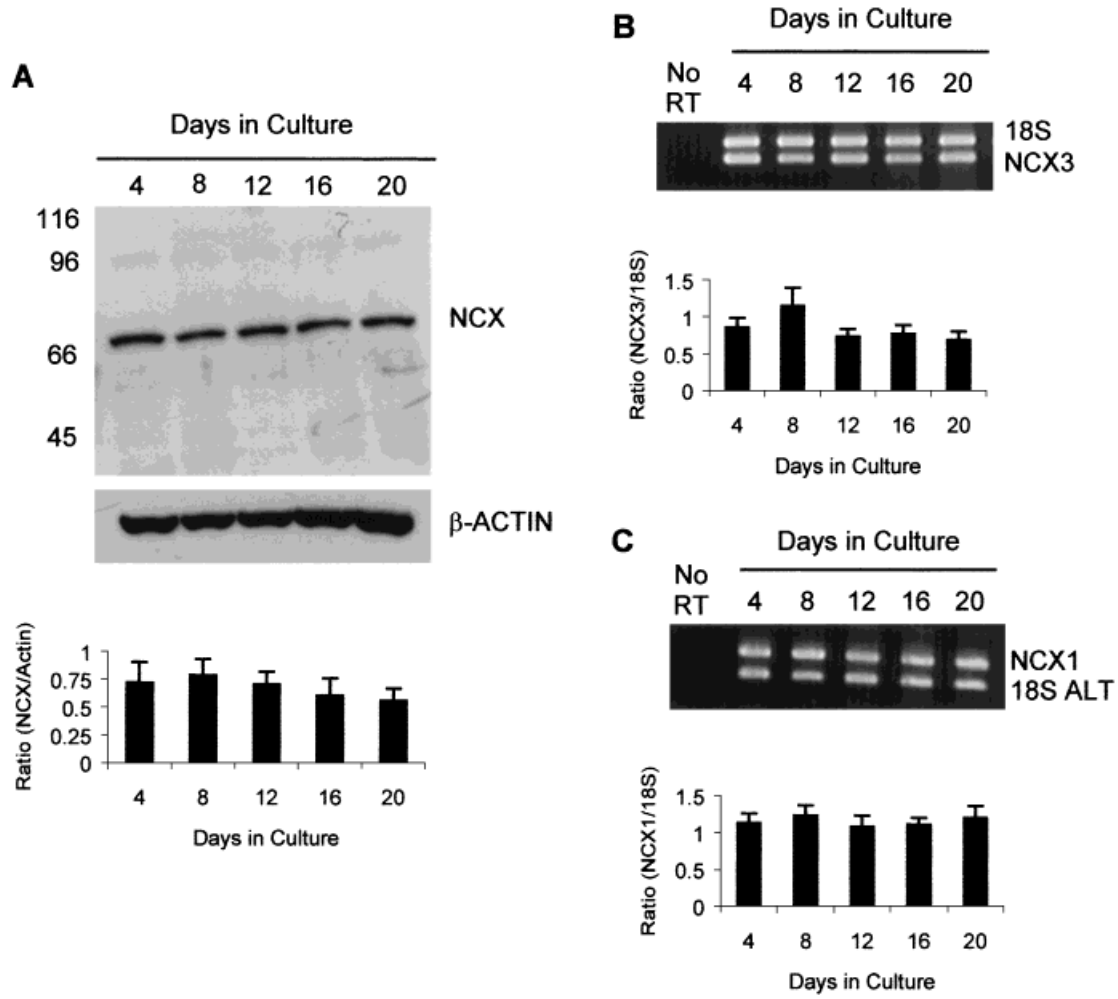

Fig. 3. Time course of NCX protein expression by cultured osteoblasts. **A**: Osteoblast plasma membrane proteins were prepared from cells cultured for 4, 8, 12, 16, or 20 days. The protein extracts (20 μg) were run on a 7.5% SDS–PAGE gel, blotted to PVDF membrane and probed with antibodies against canine cardiac NCX. A single 70 kDa product is detected. As a loading control, the blots were reprobed with antibodies against β-actin. Molecular weights (in kDa) are indicated to the left. The ratios of NCX to β-actin as determined by volume quantitation immunoblots are indicated. The level of NCX protein appears unchanged throughout the time course. The data are presented as the mean ± standard deviation (n = 3). **B**: Time course of NCX3 mRNA expression by cultured osteoblasts. Agarose gel of the products generated by relative quantitative RT-PCR from osteoblast total RNA using NCX3 gene specific primers and a 3:7 ratio of classic 18S rRNA competimer primers. The ratios of NCX3 to 18S rRNA PCR product as determined by volume quantitation are indicated (mean ± standard deviation; n = 4). **C**: Time course of NCX1 mRNA expression by cultured osteoblasts. Agarose gel of the products generated by relative quantitative RT-PCR from osteoblast total RNA using NCX1 gene specific primers and a 2:8 ratio of alternate 18S rRNA competimer primers. The ratios of NCX1 to 18S rRNA PCR product as determined by volume quantitation are indicated. The levels of both NCX1 and NCX3 message remain nearly static throughout the time course of culture (mean ± standard deviation; n = 4).

remain unchanged throughout the differentiation of the osteoblast, though a slight decrease in relative abundance of NCX is observed. It is important to note that the polyclonal NCX antibody is not isoform specific.

The expression of NCX3 mRNA was assessed during culture by relative RT-PCR with NCX3 gene specific primers. RNA was extracted from cultured osteoblasts, reverse transcribed, and then subjected to the relative RT-PCR. When normalized to the levels of 18S rRNA product, NCX message levels mimicked that of the protein, remaining relatively static throughout the differentiation of the osteoblasts though declining slightly as the cells approach day 20 in culture (Fig. 3B). NCX1 mRNA levels also remained relatively unchanged during osteoblast differentiation (Fig. 3C).

In contrast to NCX, the levels of PMCA, as determined by immunoblotting of the same plasma membrane extracts with monoclonal antibodies against a portion of human erythrocyte PMCA, show a gradual rise in PMCA that peaks at roughly the onset of mineralization (day 12), but declines rapidly by day 20, despite the continued accumulation of mineral in the cultures (Fig. 4A). The expression of PMCA mRNA, as determined by RT-PCR, likewise declines steadily over the time course of osteoblast differentiation (Fig. 4B).

NCX and PMCA Localization

Osteoblasts were examined by confocal microscopy to determine the cellular localization of NCX and PMCA. PMCA had been shown by cytochemistry to be present on the surface of the osteoblast distal from the bone matrix [Akisaka et al., 1988; Watson et al., 1989]. Previously, we have shown that NCX is deployed primarily on the surface of the osteoblast defined as apical by Ilvesaro et al. [1999], which is adjacent to bone matrix [Stains and Gay, 1998]. However, simultaneous detection of NCX and PMCA in osteoblasts has not been reported previously. As a result, co-detection of NCX and PMCA was performed to clearly define the localization of the primary calcium efflux proteins. Osteoblasts cultured for 8 days were fixed in 4% paraformaldehyde and then stained with rabbit anti-NCX and mouse anti-PMCA antibodies. BODIPY-conjugated anti-rabbit and Cy3-conjugated anti-mouse secondary antibodies allowed for the visualization of NCX as green fluorescence and PMCA as red. Z-axis sections through the cell were collected at 0.5 μm intervals using a confocal microscope. Figure 5

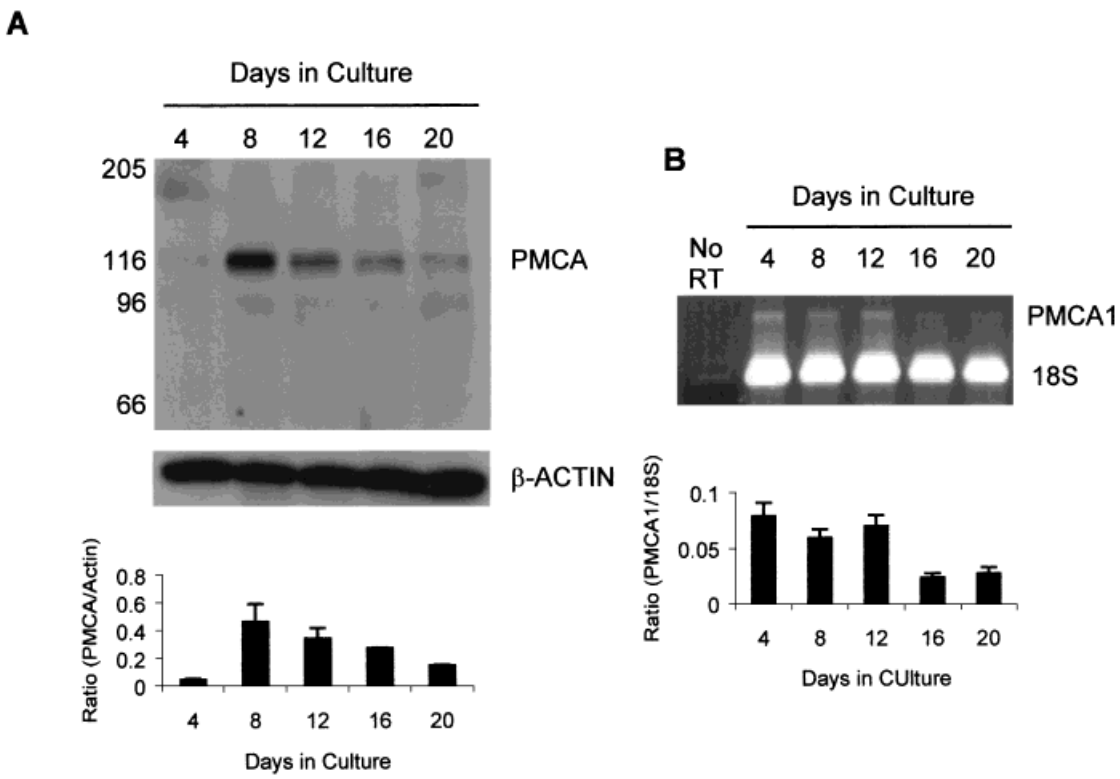

Fig. 4. Time course of PMCA protein expression by cultured osteoblasts. **A**: Osteoblast plasma membrane proteins were prepared from cells cultured for 4, 8, 12, 16, or 20 days. The protein extracts (20 μg) were run on a 7.5% SDS–PAGE gel, blotted to PVDF membrane and probed with antibodies against PMCA. A 120-kDa product corresponding to PMCA is detected. As a loading control, the blots were reprobed with antibodies against β-actin. Molecular weights (in kDa) are indicated to the left. The ratios of PMCA to β-actin as determined by volume quantitation immunoblots are indicated. PMCA protein levels peak at around day 8 in culture and diminish significantly by the 16th and 20th day. The data are presented as the mean ± standard deviation (n = 3). **B**: Time course of PMCA1 mRNA expression by cultured osteoblasts. Agarose gel of the products generated by relative quantitative RT-PCR from osteoblast total RNA using PMCA1 gene specific primers and a 1:9 ratio of classic 18S rRNA competimer primers. The ratios of PMCA1 to 18S rRNA PCR product as determined by volume quantitation are indicated. The level of PMCA1 message declines over the time course of differentiation (mean ± standard deviation; n = 3).

shows the polar distribution of PMCA and NCX in the osteoblasts, with PMCA present primarily in the z-axis sections taken at the surfaces of the osteoblasts farthest from the coverslip, while NCX was positioned almost entirely in the z-axis sections through the side of the cells adjacent to the coverslip. As expected, the staining for PMCA and NCX were both most prevalent along the plasma membrane of the osteoblasts and were in opposing membrane domains.

DISCUSSION

Osteoblast differentiation in vitro is typically divided into three stages, as reviewed by Lian and Stein [1992]. First is the proliferative phase, when the cells divide rapidly. During

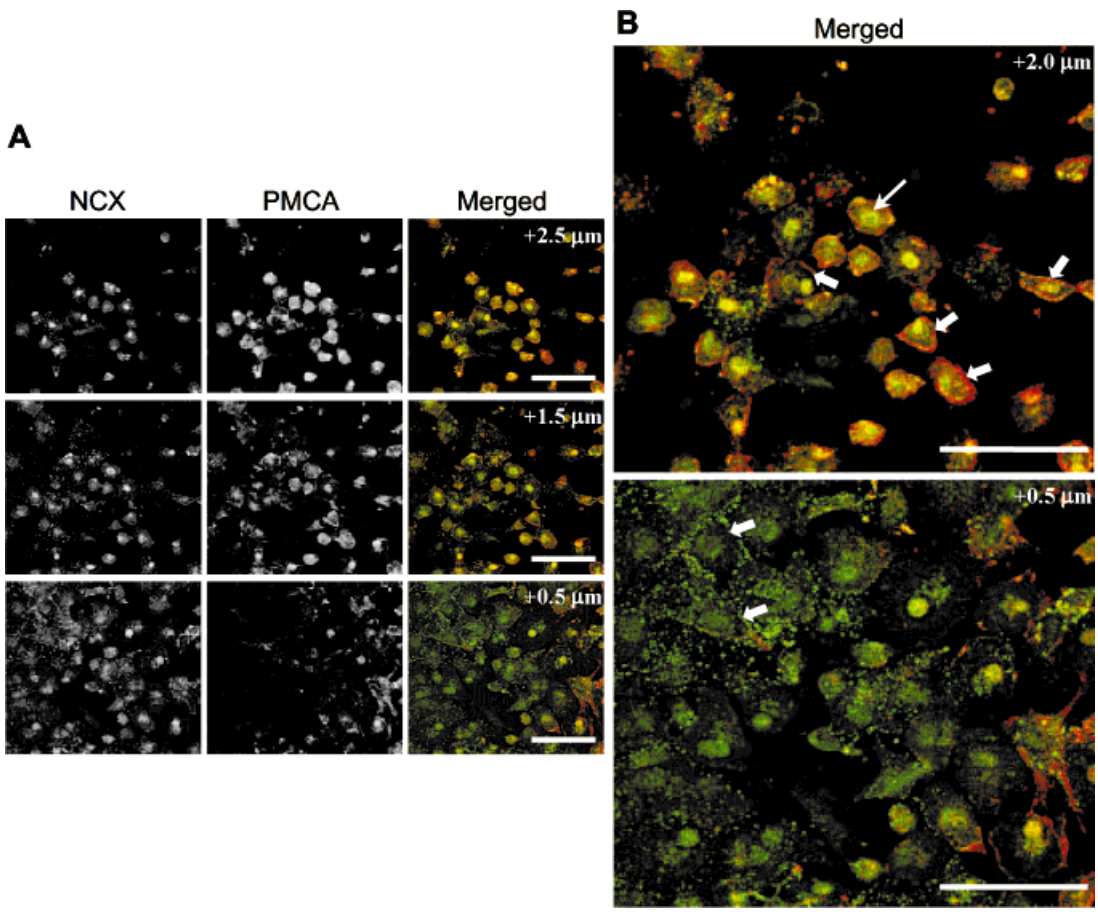

Fig. 5. Co-detection of NCX and PMCA by fluorescent confocal microscopy. Osteoblasts cultured for 8 days were fixed in 4% paraformaldehyde and then stained with antibodies against NCX and PMCA. NCX was detected using a rabbit anti-NCX polyclonal antibody and a BODIPY-conjugated goat anti-rabbit secondary antibody (green). PMCA was detected with a mouse anti-PMCA monoclonal antibody and a Cy3-conjugated secondary antibody (red). **A**: Selected confocal microscope views of Z-axis sections (X, Y plane) taken through the cells at the intervals indicated. The top panel represents an optical cross section of the cell distal to the coverslip, and the images progress down through the cell towards coverslip (bottom). The left column in each panel is the staining observed for NCX. The middle panel is the staining for PMCA. The left column is the merged image of NCX (green) and PMCA (red) staining, revealing the distribution of NCX and PMCA within the same cell. PMCA is most abundant on the plasma membrane of the cell most distal to the coverslip (+2.5 µm). NCX is deployed primarily towards the side of the cell adjacent to the coverslip (0.5 µm). Both NCX and PMCA are also observed on the lateral membranes of the cells. Scale Bar = 50 µm. **B**: Enlarged view of the merged confocal images from z-axis sections taken at 2.0 and 0.5 µm, respectively. Shown in the top panel is the distribution of PMCA (red) along the surface of the osteoblasts furthest from the coverslip. The bottom panel reveals the abundance of NCX along the surface of the osteoblast adjacent to the coverslip. The arrow at the asterisk indicates nuclear staining observed even in osteoblasts stained with non-immune antibodies and is an artifact of fixation. Thick arrows indicate the plasma membrane distribution of both NCX and PMCA. Scale Bar = 25 µm.

this phase, osteoblasts possess few of the phenotypic markers of differentiation, however, large amounts of type I collagen and fibronectin are synthesized and secreted. The second phase involves matrix maturation. Osteoblasts in this phase express markedly elevated levels of ALP and secrete bone matrix proteins, including bone sialoprotein, osteopontin, osteonectin, and low amounts of osteocalcin. The final phase of osteoblast differentiation is the mineralization phase, during which ALP levels drop, osteocalcin levels rise, and Ca^{2+} is deposited into the bone matrix.

The avian osteoblasts used in this study progress through all of these phases quite rapidly [Gay et al., 1994; Luan et al., 2000]. The data collected in these studies indicate that the cells are in the proliferative phase until approximately culture day 6, coinciding with when the cultures reach confluence. The levels of ALP continue to rise until the 12th day in culture. After the 12th day, a decline in ALP activity occurs and mineral begins to accumulate, signaling the transition from matrix maturation phase to the mineralization phase. Mineral continues to accumulate throughout the 20 day time course examined. If NCX and/or PMCA play a direct role in mineralization, then it is expected that they should be present in detectable levels during the final stages of osteoblastic differentiation when calcification of the bone matrix is occurring. NCX3 protein and mRNA were strongly expressed and remained relatively static throughout differentiation, indicating that, minimally, the exchanger is important to cellular Ca^{2+} homeostasis and is a good candidate for fostering mineralization. In contrast, PMCA protein levels, which peaks at day 8, decrease markedly during the mineralization phase, despite the continued accumulation of Ca^{2+} in the bone matrix. The reduction in expression of PMCA and its location, distal to bone matrix, argues against a role for PMCA in mineralization. The downregulation of PMCA at the onset of mineralization suggests the intriguing possibility that the disappearance of PMCA encourages the efflux of cellular Ca^{2+} through the exchanger. With Ca^{2+} efflux being apparently directed through NCX, the flow of Ca^{2+} through the osteoblasts can be fully focused on supplying the bone matrix with sufficient Ca^{2+} for apatite crystal formation.

The data presented here contain the first indication of the presence of the NCX3 isoform in osteoblasts. Further, Northern analysis and immunoblotting, using NCX1 specific antibodies have not resulted in detection of NCX1 in osteoblasts (data not shown). In fact, the PCR shown in Figure 2, while not quantitative, suggests that NCX3 is the predominant isoform of the exchanger found in osteoblasts. While few functional differences have been assigned to the NCX isoforms, NCX3 has a much more restricted tissue distribution than NCX1 [Nicoll et al., 1996; Quednau et al., 1997], which may imply a more specific function.

This is the first study that shows co-detection of NCX and PMCA in osteoblasts. When NCX and PMCA were co-detected by confocal immunocytochemistry, PMCA was distributed almost exclusively on the surfaces of the osteoblasts distal to the osteoid, while NCX was distributed on the opposing cell membrane. These obversations are consistent with our previous findings, namely, that NCX was found on the surface of the cell adjacent to bone matrix [Stains and Gay, 1998]. Further, the distribution of PMCA, as detected by immunofluorescence, matched the previously described distribution seen in vivo and in vitro by cytochemical techniques [Akisaka et al., 1988; Watson et al., 1989]. The present study is the first to confirm the polar distribution of the PMCA protein in osteoblasts (by immunocytochemistry); the previous studies were based on PMCA activity (histochemical activity). A model of PMCA and NCX distribution is presented in Figure 6.

Restricted membrane localization of NCX has been reported in other tissues. NCX has been demonstrated to be distributed solely to the basolateral surface of rabbit [Reilly et al., 1993] and rat [Yu et al., 1992; Reilly et al., 1993] renal collecting tubules and to the basolateral surface of the renal epithelial A6 cell line [Brochiero et al., 1995]. Additionally, NCX has been shown to be localized to junctional contact membranes of transverse tubules within rat cardiac myocytes [Frank et al., 1992; Kieval et al., 1992; Langer et al., 1995] and rabbit skeletal muscle [Sacchetto et al., 1996]. NCX has been localized to the basolateral membrane of gill epithelia in crustaceans [Towle, 1993; Flik et al., 1994]. Interestingly, NCX has been shown to support Ca^{2+} absorption by fish intestine [Flik et al., 1990] and to foster Ca^{2+} efflux across the basolateral plasma membranes of hepatopancreatic epithelia in lobster (*Homarus americanus*), where it is believed to play a role in the

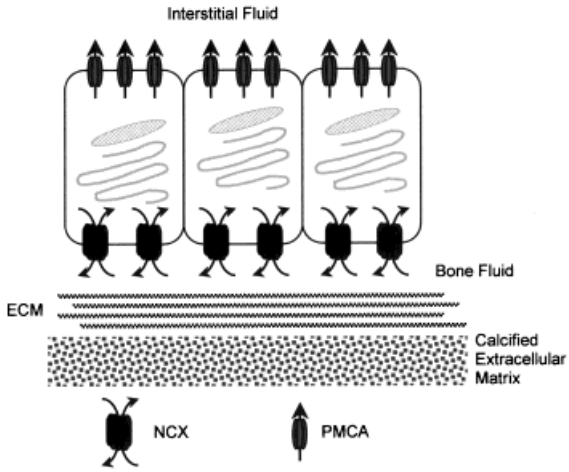

Fig. 6. Model of the polar distribution of NCX and PMCA in osteoblasts. The asymmetric positioning of the PMCA and the NCX are demonstrated. NCX is deployed mainly on the matrix-facing side of the cell. The presence of NCX on the side of the cell adjacent to sites of bone formation make NCX a candidate for a mechanism of Ca^{2+} efflux into the bone fluid for mineralization. PMCA is deployed primarily on the opposing surface of the osteoblast, opposite of the site of mineralization. Its likely role is in the maintenance of intracellular Ca^{2+} homeostasis.

transfer of Ca^{2+} to the blood in order to recalcify the exoskeleton following a molt [Zhuang and Ahearn, 1998].

Likewise, polar distribution of PMCA has been reported in other cells, including the most distal dendrites of Purkinje cells [Tolosa de Talamoni et al., 1993] and in the junctional membrane of skeletal muscle cells [Sacchetto et al., 1996]. As has been stated earlier, cytochemical techniques have also demonstrated a polar deployment of PMCA in osteoblasts [Akisaka et al., 1988; Watson et al., 1989].

Osteoblast polarity has also been demonstrated in terms of other cell functions. In addition to the well-characterized vectoral secretion of extracellular matrix from osteoblasts, the functionality of the membranes has been established by the opposed directional budding of vesicular stomata virus and influenza virus from the osteoblast [Ilvesaro et al., 1999].

PMCA has long been believed to play a role in mineralization by osteoblasts [Abramowitz and Suki, 1996]. However, its clear deployment on the surface of the osteoblast opposite to the osteoid surface of the cell and its minimal presence on the mineralizing face of the cell make the role of PMCA in the mineralization process unlikely. The primary role of PMCA may be in maintaining low intracellular Ca^{2+} concentrations within the osteoblast in support of the Ca^{2+} messenger system.

The asymmetric distribution of NCX along the membrane of osteoblasts adjacent to bone matrix concurs with a possible role for NCX in the regulation of bone fluid Ca^{2+} for mass mineralization of the bone matrix. While NCX lacks the high affinity for Ca^{2+} of PMCA, it compensates with its high capacity for Ca^{2+} efflux, making NCX a suitable Ca^{2+} efflux mechanism. This study supports our previous studies that demonstrate NCX-mediated mineralization in osteoblasts [Stains and Gay, 1998, 2001], in that NCX is expressed appropriately, and in a location consistent with that role; when specifically inhibited, mineralization ceases.

ACKNOWLEDGMENTS

We thank Virginia Gilman and Kristi Cardi for editorial assistance.

REFERENCES

Abramowitz J, Suki WN. 1996. Ca-ATPase and bone cell mineralization. Miner Electrolyte Metab 22:336–344.

Abramowitz J, Gonzalez JM, Rouse D, Suki WN. 1995. Differential expression of plasma membrane calcium pump mRNA isoforms in rat-osteoblast-like cells. Miner Electrolyte Metab 21:367–374.

Akisaka T, Yamamoto T, Gay CV. 1988. Ultracytochemical investigation of calcium-activated adenosine triphosphatase (Ca^{++}-ATPase) in chick tibia. J Bone Miner Res 3:19–25.

Anderson RE, Kemp JW, Jee WS, Woodbury DM. 1984. Ion-transporting ATPases and matrix mineralization in cultured osteoblastlike cells. In Vitro 20:837–846.

Bianco P, Riminucci M, Bonucci E, Termine JD, Gehron Robey P. 1993. Bone sialoprotein (BSP) secretion and osteoblast differentiation: Relationship between bromodeoxyuridine incorporation, alkaline phosphatase, and matrix deposition. J Histochem Cytochem 41:183–191.

Brochiero E, Raschi C, Ehrefeld J. 1995. Na/Ca exchange in the basolateral membrane of the A6 cell monolayer: Role in Ca_i homeostasis. Pflugers Arch 430:105–114.

Cai Q, Chandler JS, Wasserman RH, Kumar R, Penniston JT. 1993. Vitamin D and adaptation to dietary calcium and phosphate deficiencies increase intestinal plasma membrane calcium pump gene expression. Proc Natl Acad Sci USA 90:1345–1349.

Carafoli E. 1991. Calcium pump of the plasma membrane. Physiol Rev 71:129–153.

Flik G, Schoenmakers TJM, Groot JA, Van Os CH, Bonga SEW. 1990. Calcium absorption by fish intestine: The involvement of ATP- and sodium-dependent calcium extrusion mechanisms. J Membrane Biol 113: 13–22.

Flik G, Verbost PM, Atsma W, Lucu C. 1994. Calcium transport in gill plasma membrane of the crab *Carcinus*

maenas: Evidence for carriers driven by ATP and a Na^+ gradient. J Exp Biol 195:109–122.

Frank JS, Mottino G, Reid D, Molday RS, Philipson KD. 1992. Distribution of the Na^+–Ca^{2+} exchange protein in mammalian cardiac myocytes: An immunofluorescence and immunocolloidal gold-labeling study. J Cell Biol 117:337–345.

Gay CV, Lloyd QP. 1995. Characterization of calcium efflux by osteoblasts derived from long bone periosteum. Comp Biochem Physiol 111A:257–261.

Gay CV, Lloyd QP, Gilman VR. 1994. Characteristics and culture of osteoblasts derived from avian long bone. In Vitro Cell Dev Biol 30A:379–383.

Gerstenfeld LC, Chipman SD, Glowacki J, Lian JB. 1987. Expression of differentiated function by mineralizing cultures of chicken osteoblasts. Dev Biol 122:49–60.

Gmaj P, Murer H, Carafoli E. 1982. Localization and properties of a high affinity (Ca^{2+}+Mg^{2+})-ATPase in isolated kidney cortex plasma membranes. FEBS Lett 144:226–230.

Graf E, Penniston JT. 1981. Equimolar interaction between calmodulin and Ca^{2+}-ATPase from human erythrocyte membranes. Arch Biochem Biophys 210:257–262.

Gronowicz G, Woodiel FN, McCarthy MB, Raisz LG. 1989. In vitro mineralization of fetal rat parietal bones in defined serum-free medium: Effect of β-glycerol phosphate. J Bone Miner Res 4:313–324.

Humason GL. 1967. Animal tissue techniques. San Francisco, CA: W.H. Freeman. p 261.

Ilvesaro J, Metsikko K, Väänänen K, Tuukkanen J. 1999. Polarity of osteoblasts and osteoblast-like UMR-108 cells. J Bone Miner Res 14:1338–1344.

Jarrett HW, Penniston JT. 1977. Partial purification of the Ca^{2+} + Mg^{2+})-ATPase activator from human erythrocytes: Its similarity to the activator of 3′,5′-cyclic nucleotide phosphodiesterase. Biochem Biophys Res Commun 77:1210–1216.

Kieval RS, Bloch RJ, Lindenmayer GE, Ambesi A, Lederer WJ. 1992. Immunofluorescence localization of the Na–Ca exchanger in heart cells. Am J Physiol 263:C545–C550.

Krieger NS. 1992. Demonstration of sodium/calcium exchange in rodent osteoblasts. J Bone Miner Res 7:1105–1111.

Krieger NS. 1997. Parathyroid hormone, prostaglandin E_2, and 1,25-dihydroxyvitamin D_3 decrease the level of Na^+-Ca^{2+} exchange protein in osteoblastic cells. Calcif Tissue Int 60:473–478.

Krieger NS, Tashjian AH. 1980. Parathyroid stimulates bone resorption via a Na/Ca exchange mechanism. Nature 287:843–845.

Laemmli UK. 1970. Cleavage of structural proteins during the assembly of the head of bacteriophage T4. Nature 227:680–685.

Langer GA, Wang SY, Rich TL. 1995. Localization of the Na/Ca exchange-dependent Ca compartment in cultured neonatal rat heart cells. Am J Physiol 268:C119–C126.

Li Z, Matsuoka S, Hryshko LV, Nicoll DA, Bersohn MM, Burke EP, Lifton RP, Philipson KD. 1994. Cloning of the NCX2 isoform of the plasma membrane Na^+-Ca^{2+} exchanger. J Biol Chem 269:17434–17439.

Lian JB, Stein GS. 1992. Concepts of osteoblast growth and differentiation: basis for modulation of bone cell development and tissue formation. Crit Rev Oral Biol Med 3:269–305.

Luan YJ, Praul CA, Gay CV. 2000. Confocal imaging and timing of secretion of matrix proteins by osteoblasts derived from avian long bone. Comp Biochem Physiol 126:213–221.

Meszaros JG, Karin NJ. 1993. Osteoblasts express the PMCA1b isoform of the plasma membrane Ca(2+)-ATPase. J Bone Miner Res 10:1235–1240.

Nicoll DA, Quednau BD, Qui Z, Xia YR, Lusis AJ, Philipson KD. 1996. Cloning of a third mammalian Na^+-Ca^{2+} exchanger: NCX3. J Biol Chem 271:24914–24921.

Quednau BD, Nicoll DA, Philipson KD. 1997. Tissue specificity and alternative splicing of the Na^+/Ca^{2+} exchanger isoforms NCX1, NCX2, and NCX3 in rat. Am J Physiol 272:C1250–C1261.

Reilly RF, Shugrue CA, Lattanzi D, Briemesderfer D. 1993. Immunolocalization of the Na^+/Ca^{2+} exchanger in rabbit kidney. Am J Physiol 265:F327–F332.

Sacchetto R, Margreth A, Pelosi M, Carafoli E. 1996. Colocalization of the dihydropyridine receptor, the plasma-membrane calcium ATPase isoform 1 and the sodium/calcium exchanger to the junctional-membrane domain of transverse tubules of rabbit skeletal muscle. Eur J Biochem 237:483–488.

Shen V, Kohler G, Peck WA. 1983. A high affinity, calmodulin-responsive, (Ca^{2+}+Mg^{2+})-ATPase in isolated bone cells. Biochim Biophys Acta 727:230–238.

Short CL, Monk RD, Bushinsky DA, Krieger NS. 1994. Hormonal regulation of Na^+–Ca^{2+} exchange in osteoblast-like cells. J Bone Miner Res 9:1159–1166.

Stains JP, Gay CV. 1998. Asymmetric distribution of functional sodium–calcium exchanger in primary osteoblasts. J Bone Miner Res 13:1862–1869.

Stains JP, Gay CV. 2001. Inhibition of Na^+/Ca^{2+} exchange with KB-R7943 or bepridil diminishes mineral deposition by osteoblasts. J Bone Miner Res 16:1434–1443.

Tolosa De Talamoni N, Smith CA, Wasserman RH, Beltramino C, Fullmer CS, Penniston JT. 1993. Immunocytochemical localization of the plasma membrane calcium pump, calbindin-D_{28k}, and parvalbumin in Purkinje cells of avian and mammalian cerebellum. Proc Natl Acad Sci USA 90:11949–11953.

Towle DW. 1993. Ion transport systems in membrane vesicles isolated from crustacean tissues. J Exp Zool 265:387–396.

Turksen K, Aubin JE. 1991. Positive and negative immunoselection for enrichment of two classes of osteoprogenitor cells. J Cell Biol 114:373–384.

Watson LP, Kang Y-H, Falk MC. 1989. Cytochemical properties of osteoblast cell membrane domains. J Histochem Cytochem 37:1235–1246.

White KE, Gesek FA, Friedman PA. 1996. Na^+/Ca^{2+} exchange in rat osteoblast-like UMR 106 cells. J Bone Miner Res 11:1666–1675.

Yu ASL, Hebert SC, Lee SL, Brenner BM, Lytton J. 1992. Identification and localization of renal Na^+–Ca^{2+} exchanger by polymerase chain reaction. Am J Physiol 263:F680–F685.

Zhuang Z, Ahearn GA. 1998. Energized Ca^{2+} transport by hepatopancreatic basolateral plasma membranes of *Homarus americanus*. J Exp Biol 201:211–220.